Brief Communication | Genitourinary Imaging

http://dx.doi.org/10.3348/kjr.2015.16.2.342
pISSN 1229-6929 · eISSN 2005-8330
Korean J Radiol 2015;16(2):342-348

Korean Journal of Radiology
KJR

Multiphase Contrast-Enhanced Magnetic Resonance Imaging Features of Bacillus Calmette-Guérin-Induced Granulomatous Prostatitis in Five Patients

Hiroshi Kawada, MD[1], Masayuki Kanematsu, MD[1, 2], Satoshi Goshima, MD, PhD[1], Hiroshi Kondo, MD[1], Haruo Watanabe, MD, PhD[1], Yoshifumi Noda, MD[1], Yukichi Tanahashi, MD[1], Nobuyuki Kawai, MD[1], Hiroaki Hoshi, MD[1]

Departments of [1]Radiology and [2]Radiology Services, Gifu University Hospital, Gifu 501-1194, Japan

Objective: To evaluate the multiphase contrast-enhanced magnetic resonance (MR) imaging features of Bacillus Calmette-Guérin (BCG)-induced granulomatous prostatitis (GP).

Materials and Methods: Magnetic resonance images obtained from five patients with histopathologically proven BCG-induced GP were retrospectively analyzed for tumor location, size, signal intensity on T2-weighted images (T2WI) and diffusion-weighted images (DWI), apparent diffusion coefficient (ADC) value, and appearance on gadolinium-enhanced multiphase images. MR imaging findings were compared with histopathological findings.

Results: Bacillus Calmette-Guérin-induced GP (size range, 9–40 mm; mean, 21.2 mm) were identified in the peripheral zone in all patients. The T2WI showed lower signal intensity compared with the normal peripheral zone. The DWIs demonstrated high signal intensity and low ADC values (range, 0.44–0.68 x 10^{-3} mm^2/sec; mean, 0.56 x 10^{-3} mm^2/sec), which corresponded to GP. Gadolinium-enhanced multiphase MR imaging performed in five patients showed early and prolonged ring enhancement in all cases of GP. Granulomatous tissues with central caseation necrosis were identified histologically, which corresponded to ring enhancement and a central low intensity area on gadolinium-enhanced MR imaging. The findings on T2WI, DWI, and gadolinium-enhanced images became gradually obscured with time.

Conclusion: Bacillus Calmette-Guérin-induced GP demonstrates early and prolonged ring enhancement on gadolinium-enhanced MR imaging which might be a key finding to differentiate it from prostate cancer.

Index terms: *Granulomatous prostatitis; Multiphase contrast-enhanced MR imaging; BCG; Ring enhancement*

INTRODUCTION

Intravesical Bacillus Calmette-Guérin (BCG) immunotherapy has been employed as a treatment option for superficial urothelial carcinoma of the bladder since 1973 (1). While it is a relatively safe procedure, several complications, such as fever, granulomatous prostatitis (GP), pneumonia, hepatitis, arthralgia, and hematuria have been reported with a prevalence of 0.1–2.9% (2). Among these complications, BCG-induced GP demonstrates tumor-like morphology with an associated increase in prostate-specific antigen (PSA), resulting in an inaccurate diagnosis of a malignant tumor (2-7). It has been reported previously that magnetic resonance (MR) imaging demonstrates a diffuse decrease in signal intensity or well-circumscribed low signal intensity nodules in the peripheral zone on T2-weighted images (T2WI) (8). Suzuki et al. (9) reported non-contrast enhanced MR imaging features of BCG-induced GP in 10

Received January 24, 2014; accepted after revision November 24, 2014.

Corresponding author: Masayuki Kanematsu, MD, Department of Radiology, Gifu University Hospital, 1-1 Yanagido, Gifu 501-1194, Japan.
• Tel: (8158) 230-6439 • Fax: (8158) 230-6440
• E-mail: masa_gif@yahoo.co.jp

Korean Journal of Radiology
KJR

patients. They concluded three main findings of diffuse, nodular, and cystic with mural nodules. Thus far, no reports have focused on multiphase contrast-enhanced MR imaging features of BCG-induced GP. Therefore, the purpose of this study was to demonstrate the multiphase contrast-enhanced MR imaging features of BCG-induced GP in five patients.

MATERIALS AND METHODS

Patients

Our Institutional Review Board approved this retrospective study, and written informed consent was waived. We retrospectively searched our pathological and radiological records from June 2004 to April 2013. Five patients (age range, 60–79 years; mean age, 70.4 years) who had pathologically proven BCG-induced GP and also underwent multiphase contrast-enhanced MR imaging after BCG therapy for evaluation of bladder cancer were identified. The reference standard for the pathological diagnosis of BCG-induced GP was established using transrectal ultrasound-guided prostate needle biopsy in three patients and definitive surgery (cystprostatectomy) in two.

MR Imaging

Magnetic resonance imaging was performed using a 1.5-T system (Intera Achieva Nova Dual 1.5-T, Philips Medical Systems, the Netherlands) and an eight-channel sensitivity-encoding torso coil with a field of view of 26–28 cm. All MR imaging examinations in our study were performed primarily to evaluate the effect of BCG therapy for known bladder cancer. The MR imaging protocol consisted of a transaxial non-fat-suppressed T1-weighted turbo spin-echo sequence (repetition time [TR]/echo time [TE], 607/10; matrix size, 320 x 224; parallel imaging factor, 1.6; 5-mm section thickness with a 2-mm intersection gap; acquisition time, 20 sections in 2.5 minutes); transaxial and sagittal non-fat-suppressed T2-weighted turbo spin-echo sequence (TR/TE, 4415/100; matrix size, 320 x 224; parallel imaging factor, 1.6; 5-mm section thickness with a 2-mm intersection gap; acquisition time, 20 sections in 2 minutes for each imaging plane); spectral inversion recovery fat-suppressed diffusion-weighted image (DWI) were obtained in a transaxial plane using a single shot echo-planar sequence (TR/TE, 4000/69; parallel imaging factor, 2; b factors, 0 and 1000 s/mm^2; matrix size, 128 x 102; 5-mm section thickness with a 2-mm intersection gap; acquisition time, 20 sections in 136 seconds); and a gadolinium-enhanced fat-suppressed

Table 1. MR Imaging Features of BCG-Induced Granulomatous Prostatitis in Five Patients

Case	Age (Years)	Size (mm)	Location	Shape	PSA (ng/mL)		SI on T1WI	SI on T2WI	SI on DWI	ADC (10^{-3} mm^2/sec)	Ring Enhancement	Prolonged Enhancement	Follow-Up Period (Month)
					Before BCG Therapy	After BCG Therapy							
1	60	15 x 11 x 10	Lt. PZ & TZ	Diffuse	1.99	6.25	Slightly high	Low	High	0.56	Yes	Yes	5
2	75	24 x 20 x 14	Lt. PZ & TZ	Diffuse	≤ 0.04	5.92	Slightly high	Heterogeneous	High	0.68	Yes	Yes	49
3	61	24 x 20 x 14	Rt. PZ	Diffuse	0.42	1.81	Slightly high	Heterogeneous	High	0.62	Yes	Yes	70
4	79	9 x 8 x 6	Lt. PZ	Nodular	1.45	3.18	Slightly high	Iso-low	High	0.47	Yes	Yes	20
5	77	40 x 30 x 26	Lt. PZ & TZ	Diffuse with cystic	0.61	2.11	High	Heterogeneous	High	0.44	Yes	Yes	42

Note.— ADC = apparent diffusion coefficient, BCG = Bacillus Calmette-Guérin, DWI = diffusion-weighted image, PSA = prostate-specific antigen, PZ = peripheral zone, SI = signal intensity, TZ = transition zone, T1WI = T1-weighted image, T2WI = T2-weighted image

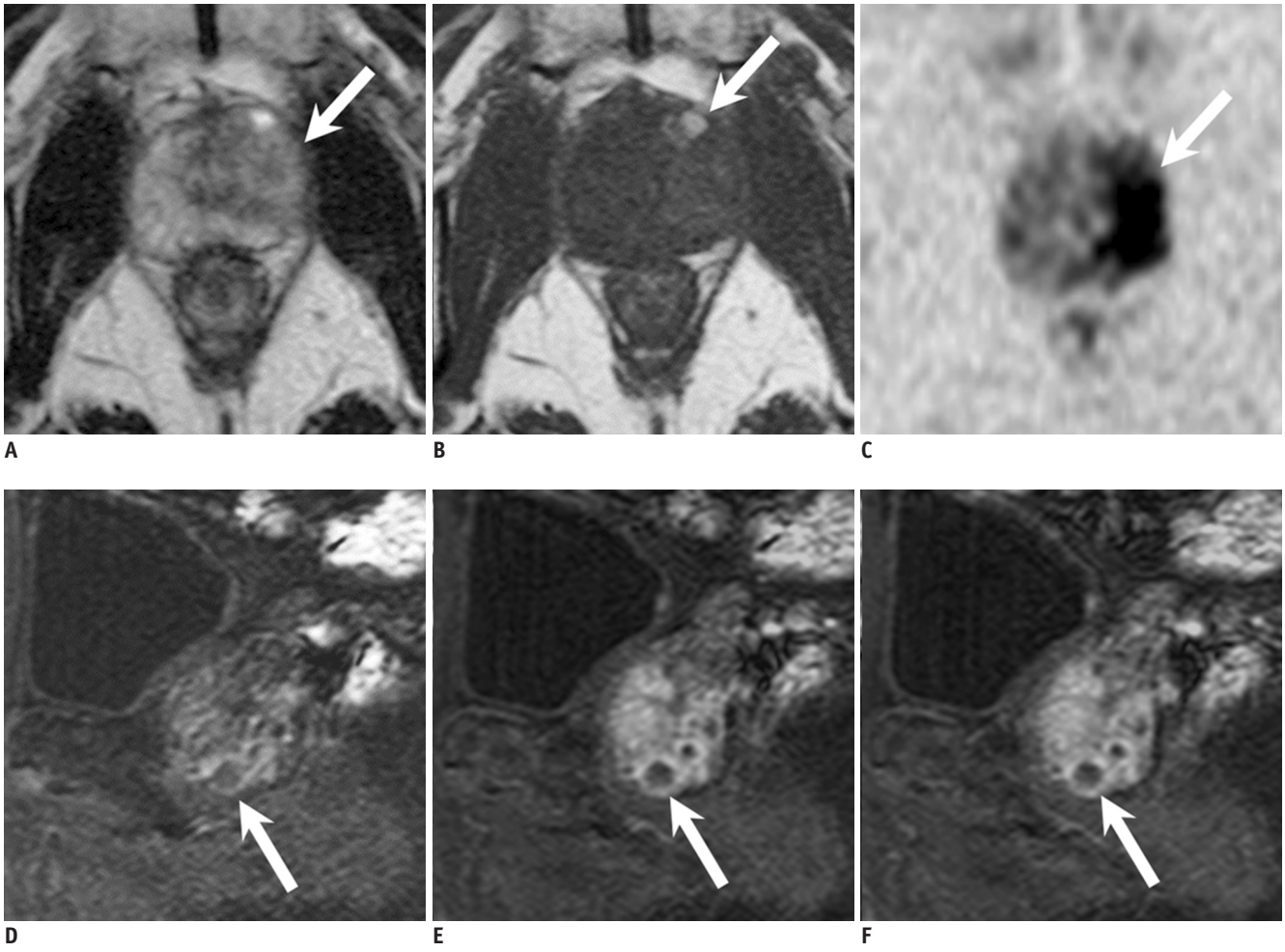

Fig. 1. 75-year-old man after Bacillus Calmette-Guérin immunotherapy for bladder carcinoma.
A. Transverse T2-weighted magnetic resonance (MR) image demonstrating heterogeneous signal mass (white arrow) in left peripheral zone of prostate extending to transition zone. **B.** Transverse T1-weighted MR image showing high signal spot (white arrow) in mass. **C.** Transverse diffusion-weighted image demonstrating restricted water diffusion in mass. Gadolinium-enhanced sagittal images obtained in arterial **(D)**, venous **(E)**, and equilibrium phases **(F)** showing early and prolonged ring enhancement in mass.

three-dimensional fast field-echo sequence (TR/TE, 10/4.1; 30° flip angle; matrix size, 272 x 163; 5-mm slice thickness with no intersectional gap; acquisition time, 20 sections in 30 seconds). A plane was set so that it intersected the urinary bladder walls at a right angle with the bladder cancer on gadolinium-enhanced MR imaging. Gadolinium-enhanced images were obtained in three temporal phases after an intravenous bolus injection of 0.1 mmol/kg of gadopentetate dimeglumine and a flush of 20 mL sterile saline solution at a rate of 3 mL/sec. The central k-space lines for the three phases were filled 30, 70, and 105 seconds after initiating the contrast injection.

Image Interpretation and Analysis

Two radiologists (with 3 and 15 years post-training experience with body MR imaging, respectively) evaluated the MR images and recorded the following findings: tumor location, lesion shape, size, signal intensity on T1-weighted images (T1WI), T2WI, and DWI, apparent diffusion coefficient (ADC) value, and multiphase contrast-enhancement pattern on gadolinium-enhanced MR images. Lesion shape and size were evaluated on T2WI according to the reports of Suzuki et al. (9). The degree of signal intensity on T1WI and T2WI was determined visually compared with that of the residual normal peripheral zone. The contrast-enhancement appearance and pattern were evaluated on arterial, venous, and equilibrium phase images.

RESULTS

Prostate-specific antigen levels increased transiently after

Korean Journal of Radiology
KJR

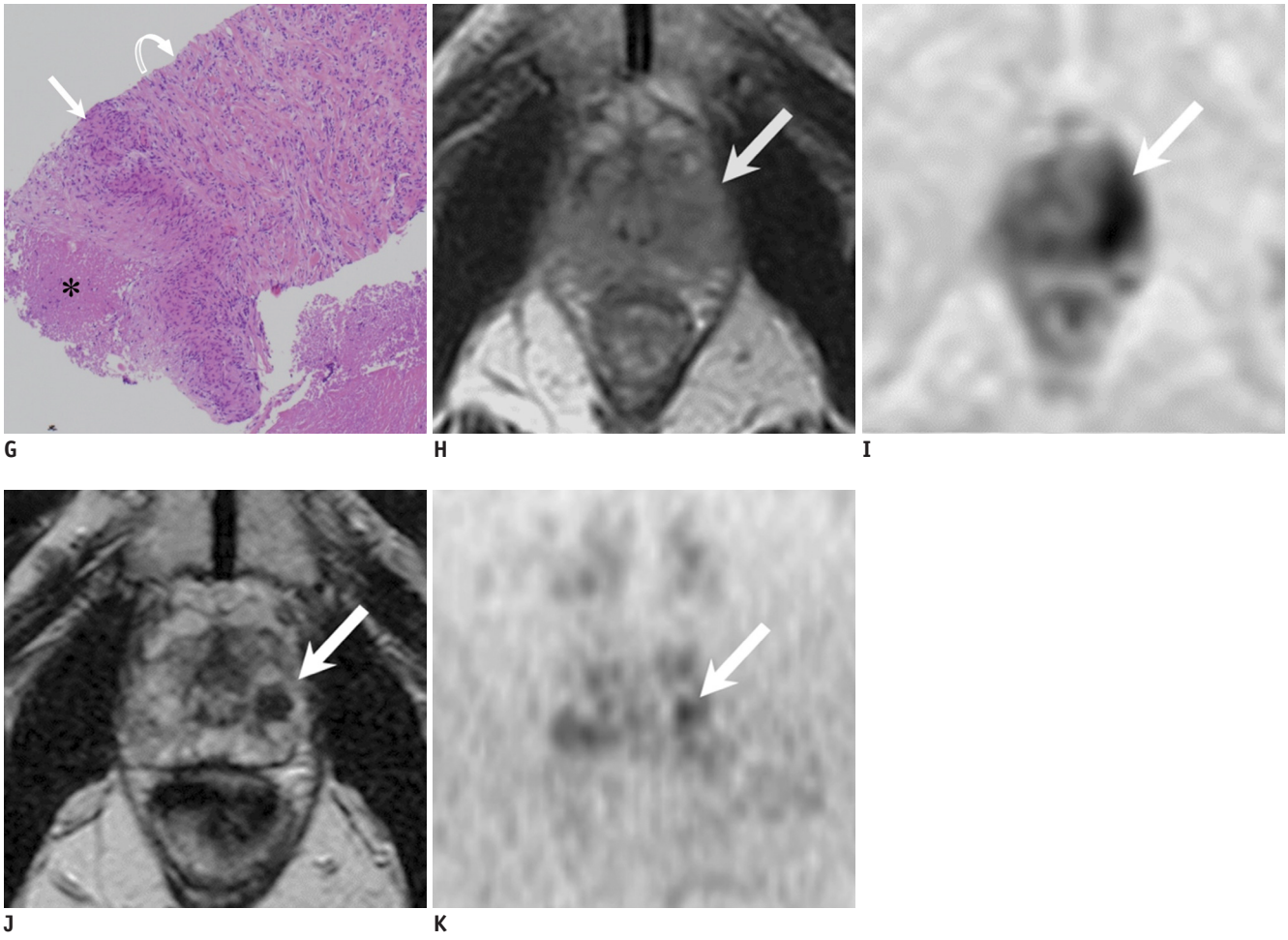

Fig. 1. 75-year-old man after Bacillus Calmette-Guérin immunotherapy for bladder carcinoma.
G. Pathological specimen obtained at biopsy (hematoxylin and eosin staining, x 100) showing granulomatous (straight arrow) and epithelioid cell (curved arrow) proliferation with central caseous necrosis (*). Transverse T2-weighted magnetic resonance (MR) image and diffusion-weighted image obtained 6 **(H, I)** and 49 months **(J, K)** after initial MR image. Mass (white arrows) shrunk in size, and diffusion signal (white arrows) decreased over time.

BCG immunotherapy in all patients. The demographic and clinical findings and MR imaging features of the patients are summarized in Table 1. The BCG-induced GP lesions were localized in the peripheral zone in all five patients and extended to the transition zone in three nodular lesions was seen in one patient, three diffuse lesions in three, and a diffuse lesion with cystic components was seen in one on T2WI. All BCG-induced lesions had lower signal intensity compared with that in the normal peripheral zone on T2WIs, except for the internal cystic components in one case. T1WIs showed slightly higher signal intensity compared to that of the normal peripheral zone, except for the internal cystic components. DWIs showed high signal intensity and low ADC values (range, 0.44–0.68 x 10^{-3} mm^2/sec; mean, 0.56 x 10^{-3} mm^2/sec), which corresponds to the GP lesions. Gadolinium-enhanced MR imaging performed in five patients showed ring enhancement in all GPs (Figs. 1-3). Granulomatous tissues with central caseation necrosis were identified by histological analysis, which corresponded to ring enhancement and a central low intensity area on gadolinium-enhanced MR imaging (Fig. 1G). Although all GPs decreased in size on follow-up MR imaging (two to six times) during a 5–70 month period, ring enhancement persisted in all GPs (Figs. 1H-K, 2G-J).

DISCUSSION

Bacillus Calmette-Guérin-induced GP has been reported to occur in at least 41% patients after BCG immunotherapy. These lesions are usually asymptomatic and require no therapy (2, 3), but may occasionally be indistinguishable from malignant tumors, such as prostate cancer or prostatic

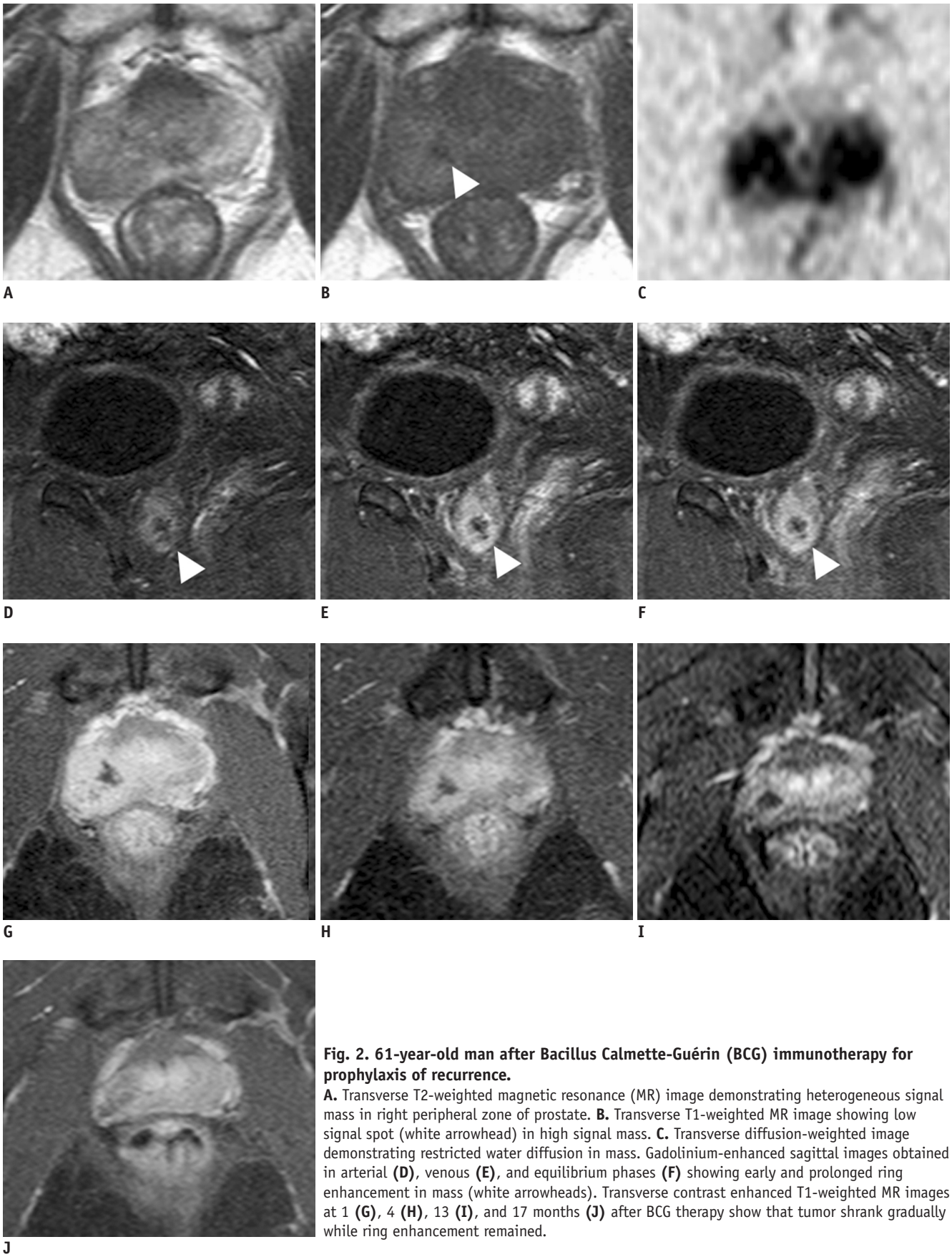

Fig. 2. 61-year-old man after Bacillus Calmette-Guérin (BCG) immunotherapy for prophylaxis of recurrence.
A. Transverse T2-weighted magnetic resonance (MR) image demonstrating heterogeneous signal mass in right peripheral zone of prostate. **B.** Transverse T1-weighted MR image showing low signal spot (white arrowhead) in high signal mass. **C.** Transverse diffusion-weighted image demonstrating restricted water diffusion in mass. Gadolinium-enhanced sagittal images obtained in arterial **(D)**, venous **(E)**, and equilibrium phases **(F)** showing early and prolonged ring enhancement in mass (white arrowheads). Transverse contrast enhanced T1-weighted MR images at 1 **(G)**, 4 **(H)**, 13 **(I)**, and 17 months **(J)** after BCG therapy show that tumor shrank gradually while ring enhancement remained.

Korean Journal of Radiology
KJR

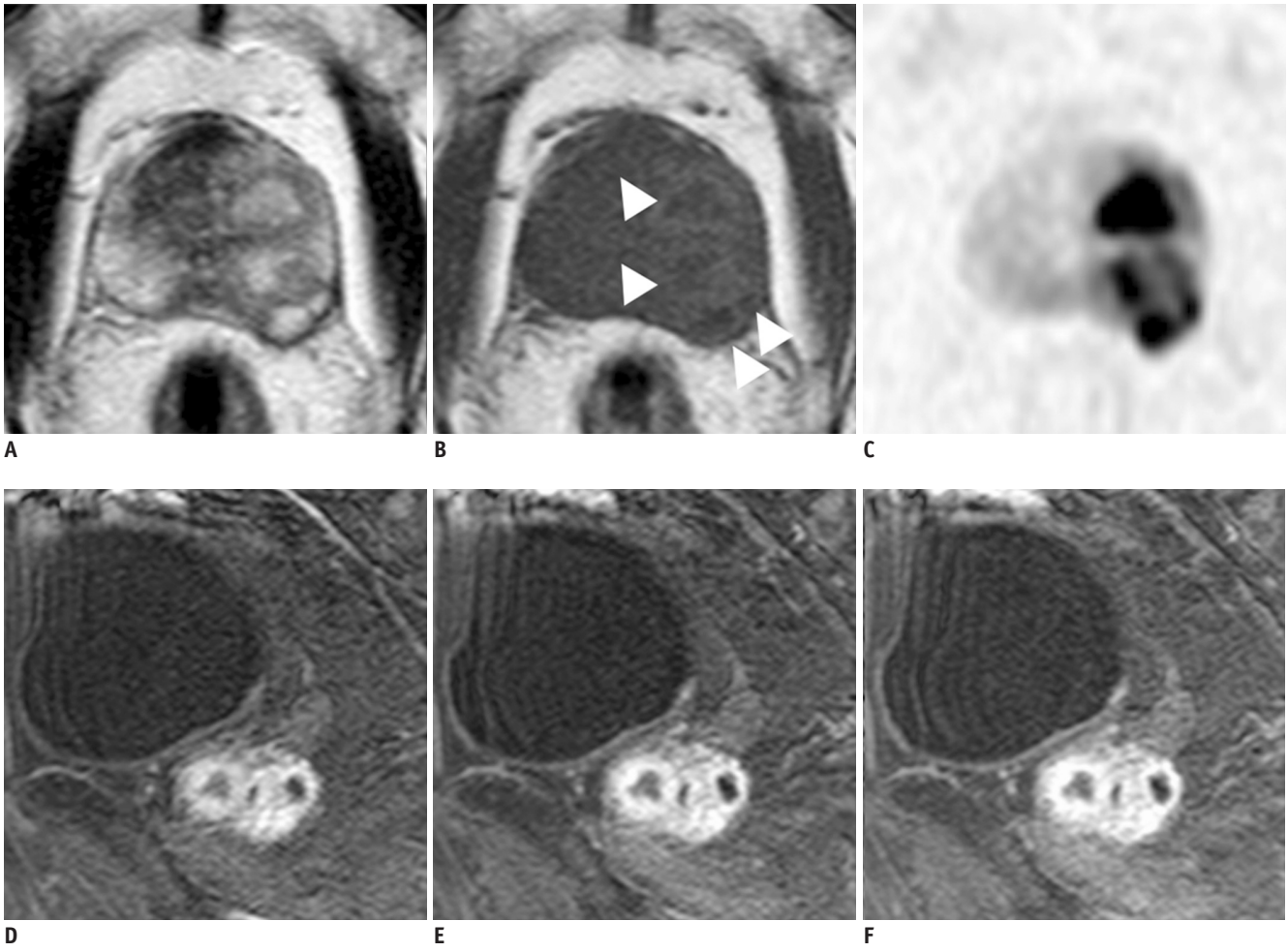

Fig. 3. 77-year-old man after Bacillus Calmette-Guérin immunotherapy for treatment of carcinoma *in situ* recurrence.
A. Transverse T2-weighted magnetic resonance (MR) image demonstrating heterogeneous signal mass in left peripheral zone of prostate extending to transition zone. **B.** Transverse T1-weighted MR image showing low signal intensity mass surrounded with slightly high signal rim (white arrowheads). **C.** Transverse diffusion-weighted image demonstrating restricted water diffusion corresponding to mass, particularly low signal area on T1-weighted image. Gadolinium-enhanced sagittal images obtained in arterial **(D)**, venous **(E)**, and equilibrium phases **(F)** showing early and prolonged ring enhancement in mass.

invasion of bladder carcinoma (4-7). BCG immunotherapy itself increases serum PSA levels, which causes difficulty differentiating BCG-induced GP from prostate cancer. A previous report demonstrated that PSA levels in patients with BCG-induced GP were 0.9–9.7 ng/mL (mean, 4.2 ng/mL) (10). In our study, PSA levels also increased after BCG immunotherapy in all cases and exceeded the upper limits of normal in three cases.

The MR imaging features of BCG-induced GP have been reported to be nonspecific (9, 11). In general, BCG-induced GP shows a tumor-like appearance with hypo-signal intensity on T2WI, similar to that of prostate cancer, in foci that involve the peripheral zone. Some studies have tried to distinguish GP from prostate cancer using MR imaging. Naik and Carey (5), who investigated transrectal ultrasound and MR imaging appearances of BCG-induced GP, concluded that neither PSA levels nor these imaging methods allow a specific diagnosis of BCG-induced GP to be established or differentiated from prostate cancer (5). In our cases, we observed early and prolonged ring enhancement on gadolinium-enhanced multiphase MR imaging, which is characteristic of BCG-induced GP. According to previous reports, extrapulmonary macronodular tuberculoma commonly appears as an unenhanced, hypointense mass with slight enhancement at the periphery of the mass on contrast-enhanced MR imaging (12-14). These findings reflect the histological differences between central caseating necrosis and peripheral granulomatous tissues. Engin et al. (12) reported that peripheral ring enhancement on MR imaging can be useful to differentiate a tuberculous

prostatic abscess from a malignant tumor. In contrast, microvessel alterations and neovascularity predominantly occurs in prostate cancer compared with other pathologies of the prostate, such as benign hyperplasia or prostatic intraepithelial neoplasia (15). Increased tumor vascularity leads to early enhancement and rapid washout of contrast material from the prostate cancer compared with that of normal prostate tissue (16).

All BCG-induced GP lesions in our study showed a decrease in size over time, which also could be used to differentiate BCG-induced GP from prostate cancer. In addition, Bour et al. (11) reported that repeat imaging after 1 year of antituberculous treatment results in a return to normal appearance of the prostate gland with no detectable residual cavity.

Our study had several limitations. First, although we believe that ring enhancement and the decrease in size over time could be used to distinguish BCG-induced GP from prostate cancer, we were unable to directly assess the diagnostic performance of these MR imaging findings as we did not compare them with prostate cancers in this study. Further clinical studies are required to confirm the diagnostic performance of contrast-enhanced multiphase MR imaging features of BCG-induced GP for the differential diagnosis. Second, MR imaging was performed primarily to evaluate the effect of BCG therapy on bladder cancer, so the MR imaging parameters including slice thickness and slice plane were not specifically optimized for evaluating BCG-induced GP.

In conclusion, multiphase contrast-enhanced MR imaging can be a useful modality to distinguish BCG-induced GP from other prostate cancers. Early and prolonged ring enhancement is a possible MR imaging finding to differentiate BCG-induced GP from prostate cancer.

REFERENCES

1. Morales A, Eidinger D, Bruce AW. Intracavitary Bacillus Calmette-Guerin in the treatment of superficial bladder tumors. *J Urol* 1976;116:180-183
2. Lamm DL, Stogdill VD, Stogdill BJ, Crispen RG. Complications of bacillus Calmette-Guerin immunotherapy in 1,278 patients with bladder cancer. *J Urol* 1986;135:272-274
3. Oates RD, Stilmant MM, Freedlund MC, Siroky MB. Granulomatous prostatitis following bacillus Calmette-Guerin immunotherapy of bladder cancer. *J Urol* 1988;140:751-754
4. Miyashita H, Troncoso P, Babaian RJ. BCG-induced granulomatous prostatitis: a comparative ultrasound and pathologic study. *Urology* 1992;39:364-367
5. Naik KS, Carey BM. The transrectal ultrasound and MRI appearances of granulomatous prostatitis and its differentiation from carcinoma. *Clin Radiol* 1999;54:173-175
6. Gevenois PA, Stallenberg B, Sintzoff SA, Salmon I, Van Rogemorter G, Struyven J. Granulomatous prostatitis: a pitfall in MR imaging of prostatic carcinoma. *Eur Radiol* 1992;2:365-367
7. Takeuchi M, Suzuki T, Sasaki S, Ito M, Hamamoto S, Kawai N, et al. Clinicopathologic significance of high signal intensity on diffusion-weighted MR imaging in the ureter, urethra, prostate and bone of patients with bladder cancer. *Acad Radiol* 2012;19:827-833
8. Ma W, Kang SK, Hricak H, Gerst SR, Zhang J. Imaging appearance of granulomatous disease after intravesical Bacille Calmette-Guerin (BCG) treatment of bladder carcinoma. *AJR Am J Roentgenol* 2009;192:1494-1500
9. Suzuki T, Takeuchi M, Naiki T, Kawai N, Kohri K, Hara M, et al. MRI findings of granulomatous prostatitis developing after intravesical Bacillus Calmette-Guérin therapy. *Clin Radiol* 2013;68:595-599
10. Oppenheimer JR, Kahane H, Epstein JI. Granulomatous prostatitis on needle biopsy. *Arch Pathol Lab Med* 1997;121:724-729
11. Bour L, Schull A, Delongchamps NB, Beuvon F, Muradyan N, Legmann P, et al. Multiparametric MRI features of granulomatous prostatitis and tubercular prostate abscess. *Diagn Interv Imaging* 2013;94:84-90
12. Engin G, Acunaş B, Acunaş G, Tunaci M. Imaging of extrapulmonary tuberculosis. *Radiographics* 2000;20:471-488; quiz 529-530, 532
13. Fan ZM, Zeng QY, Huo JW, Bai L, Liu ZS, Luo LF, et al. Macronodular multi-organs tuberculoma: CT and MR appearances. *J Gastroenterol* 1998;33:285-288
14. Kawamori Y, Matsui O, Kitagawa K, Kadoya M, Takashima T, Yamahana T. Macronodular tuberculoma of the liver: CT and MR findings. *AJR Am J Roentgenol* 1992;158:311-313
15. Padhani AR, Harvey CJ, Cosgrove DO. Angiogenesis imaging in the management of prostate cancer. *Nat Clin Pract Urol* 2005;2:596-607
16. Bonekamp D, Jacobs MA, El-Khouli R, Stoianovici D, Macura KJ. Advancements in MR imaging of the prostate: from diagnosis to interventions. *Radiographics* 2011;31:677-703